Author Manuscript

Author Manuscript

Author Manuscript

Author Manuscript

HHS Public Access

Author manuscript

J Comp Neurol. Author manuscript; available in PMC 2015 September 14.

Published in final edited form as:

J Comp Neurol. 2012 July 1; 520(10): 2256–2274. doi:10.1002/cne.23060.

Connexin 57 Is Expressed by the Axon Terminal Network of B-type Horizontal Cells in the Rabbit Retina

Feng Pan, **Joyce Keung**, **In-Beom Kim**, **Mark B. Snuggs**, **Stephen L. Mills**, **John O'Brien**, and **Stephen C. Massey***

Department of Ophthalmology and Visual Science, University of Texas Medical School at Houston, Houston, Texas 77030

Abstract

In the rabbit retina there are two types of horizontal cell (HC). A-type HCs (AHC) are axonless and extensively coupled via connexin (Cx)50 gap junctions. The B-type HC (BHC) is axon-bearing; the somatic dendrites form a second network coupled by gap junctions while the axon terminals (ATs) form a third independent network in the outer plexiform layer (OPL). The mouse retina has only one type of HC, which is morphologically similar to the B-type HC of the rabbit. Previous work suggested that mouse HCs express Cx57 (Hombach et al. [2004] Eur J Neurosci 19:2633–2640). Therefore, we cloned rabbit Cx57 and raised an antibody to determine the distribution of Cx57 gap junctions among rabbit HCs. Dye injection methods were used to obtain detailed fills for all three HC networks for analysis by confocal microscopy. We found that Cx57 was associated with the B-type AT plexus. Cx57 plaques were anticorrelated with the B-type somatic dendrites and the A-type HC network. Furthermore, there was no colocalization between Cx50 and Cx57. We conclude that in the rabbit retina, Cx57 is only found on BHC-AT processes. Thus, in species where there are two types of HC, different connexins are expressed. The absence of Cx57 labeling in the somatic dendrites of B-type HCs suggests the possibility of an additional unidentified HC connexin in the rabbit.

INDEXING TERMS

connexin 57; horizontal cells; retina; rabbit

Although chemical neurotransmission is the dominant form of neuronal communication in the central nervous system, there are also many electrical synapses, or gap junctions (Connors and Long, 2004). Gap junctions are composed of two docked hemichannels called connexons. Each connexon, or hemichannel, is built from six connexins surrounding a central pore. This pore forms an intercellular channel between the connected cells that allows the passage of ions and small molecules up to a molecular weight of ≈1,000 Da. (Vaney and Weiler, 2000; Goodenough and Paul, 2003; Menichella et al., 2003). Approximately 20 different connexins have been identified in mammals but only a small subset are expressed in neurons (Willecke et al., 2002). It has been established that gap

*CORRESPONDENCE TO: Stephen C. Massey, Department of Ophthalmology and Visual Science, University of Texas Medical School at Houston, 6431 Fannin, Houston TX 77030. steve.massey@uth.tmc.edu.

Author Manuscript Author Manuscript Author Manuscript Author Manuscript

junctions are essential components of certain retinal circuits. For example, AII amacrine cells express Cx36 and in the Cx36 knockout mouse, there is a major deficit such that rod-driven ON responses are absent (Deans et al., 2002).

In mammals, most species have two morphologically distinct types of horizontal cells (HCs) (Masland, 2001). In the rabbit, these are called A- and B-type HCs. A-type HCs are large axonless cells, which contact cones exclusively. They are the best-coupled cells in the retina, passing both Lucifer Yellow and Neurobiotin, and they are connected via Cx50 gap junctions, some of which form giant plaques (O'Brien et al., 2006). In contrast, B-type HCs are axon-bearing cells; the end of the axon expands into a complex branching structure known as the B-type axon terminal (B-type AT). The somatic dendrites also contact cones, whereas the axon terminal branch endings contact rods (Nelson et al., 1975; Dacheux and Raviola, 1982; Pan and Massey, 2007). Both the somatic dendrites and the axon terminal are independently coupled and also electrically isolated from one another so that, functionally, there are three horizontal networks in the outer plexiform layer (OPL) (Dacheux and Raviola, 1982; Vaney, 1993; Mills and Massey, 1994; Pan and Massey, 2007). B-type HCs do not pass Lucifer Yellow, which indicates the presence of a connexin different than in the A-type HC network (Mills and Massey, 1994, 2000). However, the connexins expressed by B-type HCs in the rabbit retina have not been identified.

Surprisingly, in rat and mouse retinae there is only one type of HC, which resembles the B-type axon-bearing HC of the rabbit (Peichl and Gonzalez-Soriano, 1994). There is strong evidence that mouse HCs express Cx57 (Hombach et al., 2004). In fact, the expression of Cx57 may be restricted to retinal HCs (Hombach et al., 2004), although traces have also been reported for olfactory bulb and cerebellum (Zappala et al., 2010; Zhang, 2011). Furthermore, in Cx57 knockout mice dye coupling in HCs was dramatically reduced and the diameter of the HC receptive field was reduced (Shelley et al., 2006). The deletion of Cx57 also produced behavioral consequences consistent with the absence of HC coupling (Pandarinath et al., 2010). Expression studies have shown that Cx57-GFP transfected cells formed gap junction plaques at their contact points. These Cx57 channels had a unitary conductance of 57pS and were strongly modulated by pH (Palacios-Prado et al., 2009). Previous results suggest that Cx57 is also expressed in the rabbit OPL (Puller et al., 2009).

The rabbit retina presents an interesting opportunity to compare the expression of gap junction proteins among different HC types. In this study we developed a new antibody against rabbit Cx57 and we report the distribution of Cx57 labeling in the rabbit retina. By targeting specific structures in the OPL, we have filled each of the three HC networks and we find that Cx57 is located only in the B-type AT network. This confirms that different HC types express different connexins. Of the three HC networks in the OPL, A-type HCs express Cx50 and B-type ATs use Cx57, while the connexin responsible for coupling in the B-type soma network has not been identified. These results differ from a recent report in mouse retina, where both dendrites and axon terminals of axon-bearing HCs were immunopositive for Cx57 (Janssen-Bienhold et al., 2009).

Author Manuscript Author Manuscript Author Manuscript Author Manuscript

MATERIALS AND METHODS

Preparation of isolated retina

The preparation has previously been described in detail (Massey and Mills, 1999). A brief summary is provided here. Under a protocol approved by the Institutional Animal Welfare Committee, adult New Zealand Albino white rabbits of either sex (2–3 kg) were deeply anesthetized with urethane (loading dose, 1.5 g/kg, intraperitoneal) and the orbit was infused with 2% lidocaine hydrochloride before enucleation. The eye was then removed and hemisected. The retina was isolated from the inverted eyecup while immersed in oxygenated Ames medium. Retinal cells were prelabeled with 4,6-diamino-2-phenylindole (DAPI) by incubating in Ames medium with 5 μM DAPI for 30 minutes.

Cloning of Cx57 from rabbit retina

Total RNA was extracted from rabbit retina using an RNeasy Mini kit (Qiagen, Valencia, CA). First-strand cDNA was made by reverse transcription with oligo(dT) primer and Superscript III First-Strand Synthesis System (Invitrogen, Rockville, MD). Two overlapping fragments of rabbit Cx57 were amplified using two primer pairs (forward: 5′-ATGGGAGATTGGAATTTACTGGGTG-3′; 5′-GCTGCTGAGGACGTCTGGGATGA-3′; reverse: 5′-GCGCAGCAGACATCCTTTCAGAG-3′; 5′-GGCCTTGCGACTTCCTGGGCCTAATC-3′) designed from highly conserved regions of human and mouse Cx57. 3′ Race polymerase chain reaction (PCR) was performed using a 3′ Race System (Invitrogen) with a specific primer from rabbit Cx57 (5′-GAGTGGGGGCTGGGTAGACAAATC-3′) to obtain the c-terminal cDNA. One hundred fifty nanograms of first-strand cDNA was amplified with 35 cycles of PCR by using 100 pmol of each primer. PCR products were gel-purified and cloned into pGEM-T vectors (Promega, Madison, WI). The cDNA clones were sequenced on both strands and the sequence was analyzed using GeneRunner (Hastings Software, Minneapolis, MN), BLAST (National Center for Biotechnology Information, Bethesda, MD), Lasergene (DNASTAR, Madison, WI), Clustal X (Semple-Rowland et al., 1999), and Phylip (Felsenstein, 1995) software.

A fusion protein of rabbit Cx57, amino acids 335–393, containing the immunogen sequence was created by His-Patch ThioFusion Expression (Invitrogen, Carlsbad, CA). Western blot analysis of the fusion protein using the Anti-Thio antibody recognized recombinant thioredoxin proteins from the His-Patch with the Cx57 peptides inserted at the active site.

The full coding sequence of rabbit Cx57 was subcloned into GFP Fusion TOPO vector (Invitrogen). Two μg of the Cx57-GFP plasmid DNA was used for the transient transfection of Hela cells. For Cx57 antibody labeling, the transfected Hela cells were blocked with 10% donkey serum / 20 mM phosphate buffer (PB) / 0.45 M NaCl for 30 minutes at room temperature and incubated in the rabbit Cx57 antibody 1:500, mouse GFP 1:100, Alexa Fluor 633-phalloidin (Invitrogen, Cat. no. A22284) 1:50, to label actin filaments, with 1% donkey serum / 0.3% Triton X-100 / 20 mM PB / 0.45 M NaCl at 4°C overnight. Then the cells were rinsed several times in 20 mM PB / 0.45 M NaCl and incubated in the secondary antibodies, donkey antirabbit Cy3 1:200 and donkey antimouse Alexa 488 1:200 for 30

Author Manuscript Author Manuscript Author Manuscript Author Manuscript

minutes at room temperature, then rinsed again and mounted in Vectashield (Vector Laboratories, Burlingame, CA) for viewing.

Development of anti-Cx57 antibodies

Polyclonal antisera were raised in rabbits against a synthetic peptide corresponding to the C-terminal amino acids 414–430 (CRESGGWVDKSRPGSRKA) of rabbit Cx57. This sequence is 90% similar to human and mouse. The peptide synthesis, conjugation to keyhole limpet hemocyanin, immunizations, and bleeds were performed by Bethyl Laboratories (Conroe, TX). Bleeds were tested by western blots against bacterially expressed GST fusion proteins containing the C-terminal domain of rabbit Cx57 and immunostaining in fixed rabbit retina.

Bleeds with good titers of anti-Cx57 antibodies were used for affinity purification. The Cx57 C-terminal peptide was coupled to a 2 ml SulfoLink gel column (Pierce, Rockford, IL) via the N-terminal cysteine sulfhydryl group. Approximately 30 ml sera containing anti-Cx57 antibodies were gravity-fed over the column twice. The column was washed with 50 column volumes of borate buffered saline solution (1 M NaCl, 100 mM boric acid, 20 mM Na borate, 0.1% Tween-20) and once with 10 ml 75 mM HEPES pH 7.2 and then eluted by the addition of 15 ml of elution buffer (75 mM HEPES pH 7.2, 25% ethylene glycol, 3.0 M $MgCl_2$). The eluted antibody was dialyzed against DPBS (137 mM NaCl, 2.7 mM KCl, 10 mM Na_2HPO_4, 1.5 mM KH_2PO_4, pH 7.4) and then concentrated with a 15 kDa Centriprep centrifugal filtration device (Millipore, Bedford, MA). Sodium azide was added to 0.05% and antibody stored at 20°C.

Monoclonal antibody production

Monoclonal antibodies were developed in Balb/c mice using a protocol approved by the University of Texas Health Science Center, Houston institutional Animal Welfare Committee. Four-week-old female Balb/c mice were injected with the Cx57 C-terminal peptide (Bethyl Labs) conjugated to KLH through 5′-sulfhydryl group linkage. The conjugate diluted into sterile PBS was emulsified with MPL+TDM emulsion (Sigma, St. Louis, MO) to a final concentration of 15 μg/100 μl. Mice were injected subcutaneously with 200 μl on day 1 and boosted on day 14. The mice were then test-bled on day 24. Test bleeds were first screened by enzyme-linked immunosorbent assay (ELISA) against the peptide antigen. Positive test bleeds were further evaluated by immunostaining fixed rabbit retina.

Three weeks after the last boost, positive staining mice were given the final boost intravenously. Four days later the spleen was removed and fused to SP2/0Ago14 (Sp2) cells (ATCC, Manassas, VA; CRL-1581) using 1500 molecular weight polyethylene glycol (PEG). Hybridoma culture medium was screened by ELISA. Positive wells were further evaluated by immunolabeling in fixed rabbit retina. Samples that indicated staining within the OPL were cloned twice by limiting dilution and isotype was determined to be IgG1 using monoclonal isotyping reagents from Sigma. The clonal population was maintained in Dulbecco’s modified Eagle’s medium (DMEM) supplemented with 10% fetal bovine serum (FBS) in a 10% CO_2 37°C humidified incubator. Cells were grown in a T-75 flask and

Author Manuscript Author Manuscript Author Manuscript Author Manuscript

media containing Cx57 antibody was stored at −80°C until affinity purification, as described above.

Dye injection of Neurobiotin

Details of this procedure have been published previously (Pan and Massey, 2007) based on procedures first reported for retina by Vaney (1991). Briefly, pieces of retina prelabeled with DAPI were visualized on an Olympus BX-50WI microscope (Tokyo, Japan) equipped with epifluorescence. Cells were impaled under visual control by using pipettes tip filled with 4% Neurobiotin (Vector Laboratories) and 0.5% Lucifer Yellow-CH (Molecular Probes, Eugene, OR) in ddH_2O, then backfilled with 3 M LiCl. Alexa568 (Molecular Probes, A10437) was backfilled with 3 M KCl. The electrode resistance was ≈100 MΩ. The impaled cells were injected with a biphasic current (±1.0 nA, 3 Hz) for 10 minutes. After the last injection the retinal pieces were fixed in 4% paraformaldehyde for at least 10 minutes before further immunocytochemical experiments. In some experiments, meclofenamic acid (200 lM; Sigma, M-4531) was used to block gap junctions (Pan et al., 2007).

Immunocytochemistry

After fixation the tissues were washed extensively with 0.1 M PB, pH 7.4, and blocked with 3% donkey serum in 0.1 M PB with 0.5% Triton-X 100 and 0.1% NaN_3 overnight. The primary antibodies, listed in Table 1, were diluted in 0.1 M PB with 0.5% Triton-X100 and 0.1% NaN_3 containing 1% donkey serum. The tissues were incubated for 3–7 days at 4°C and, after extensive washing, incubated in secondary antibodies overnight at 4°C. After washing with 0.1 M PB the tissues were mounted in Vectashield (Vector Laboratories) for observation.

The secondary antibodies used were donkey antirabbit or antigoat Cy-3 (1:200) and donkey antimouse or anti-goat Cy-5 (1:200) (Jackson ImmunoResearch Laboratories, West Grove, PA). Neurobiotin was visualized with Alexa-488 conjugated streptavidin (Molecular Probes) or Cy3-conjugated streptavidin (Jackson ImmunoResearch Laboratories).

For immuno-electron microscopy, retinal sections were stained as above but without Triton X-100 and sodium azide and then post-fixed in 1% glutaraldehyde for 1 hour and in 1% osmium tetroxide for 1 hour. Sections were washed through a graded series of alcohol, stained with 1% uranyl acetate and embedded in Epon 812. Ultrathin sections were examined with an electron microscope (Jeol 1200EX).

Antibody characterization

The primary antibodies used in this study are listed in Table 1. A monoclonal mouse antibody against green fluorescent protein (GFP) was purchased from ClonTech (Mountain View, CA; Cat. no. 632381). The antibody was produced against full-length *Aequorea victoria* GFP (AcGFP). The specificity was confirmed by western blot analysis using lysate made from a HEK 293 cell line stably expressing AcGFP1. A band of ≈30 kDa corresponding to AcGFP1 was observed in the lane loaded with the AcGFP1 cell lysate. A band of this size was not detected in the lysate of untransfected HEK 293 cells.

Author Manuscript Author Manuscript Author Manuscript Author Manuscript

A rabbit polyclonal antibody against mGluR6 was raised against a C-terminal peptide, the final 19 residues (KTTSTVAAPPKGADTEDPK), and a goat polyclonal antibody was raised against an N-terminal peptide, 362–375 (KLTSSGGQSDEATR), respectively, of the rabbit mGluR6 sequence. The two antibodies double-labeled the same punctate structures in the OPL, consistent with the known location of mGluR6 receptors at the dendritic tips of rod bipolar cells and ON cone bipolar cells (Vardi et al., 2000; Li et al., 2004; Pan et al., 2007).

A mouse monoclonal antibody against RIBEYE recombinant protein consisting of amino acid (aa) sequence 361–445 of C-terminal binding protein 2 (Ctbp2), a RIBEYE homolog, was purchased from BD Biosciences (San Diego, CA; No. 612044; 1:500). The antibody was generated against mouse Ctbp2 and it recognizes synaptic ribbons in mammalian retinas (Schmitz et al., 2000; tom Dieck et al., 2005). The staining patterns for Ctbp2 antibodies in the mammalian retina are well known.

An antibody against calbindin 28 kDa (CB-38, Swant, Bellinzona, Switzerland) was reported by the manufacturer to stain the appropriate 27–28-kDa band in immunoblots from brain tissue of rat, chicken, monkey, and mouse. This antibody labeled HCs and a specific type of bipolar cell in rabbit retina as previously reported (Massey and Mills, 1996).

A rabbit polyclonal antibody made against a 19 aa peptide sequence (340–358) within the C-terminal cytoplasmic domain of mouse Cx40 (Chemicon/Millipore, AB1726) crossreacts with Cx50-CT. This antibody stained large Cx50 gap-junction plaques on A-type HCs in the rabbit retina as previously reported (O'Brien et al., 2006; Puller et al., 2009).

Rabbit anti-Cx57 (C-term) (Invitrogen, Zymed, Cat. no. 40-4800) is a polyclonal antibody raised against mouse (rat) connexin 57 (C-term) (aa 434–446) (Ciolofan et al., 2007). Anti-connexin 57 (C-term) recognizes the expressed product of the Gja10 gene. This antibody is specific for the C-terminal region of the connexin 57 protein. On western blots it identifies bands at ≈54 kDa (Cx57) as well as other unidentified bands. This antibody produced punctate labeling of Cx57 in the OPL of the mouse retina. Unfortunately, this labeling pattern was also present in the Cx57 knockout mouse (Ciolofan et al., 2007).

Rabbit anti-Cx57 (Mid) (Invitrogen, Zymed, Cat. no. 40-5000) is a polyclonal antibody against a peptide derived from an internal region of the mouse Cx57 (aa 248–263) (Ciolofan et al., 2007). This antibody is specific for an internal region of Cx57 protein. On western blots it identifies a target band at ≈54 kDa as well as other unidentified bands. This antibody produced punctate labeling of Cx57 in the OPL of the mouse retina that was absent in the Cx57 knockout mouse (Ciolofan et al., 2007).

Confocal microscopy

Images were acquired on a Zeiss LSM-510 (Thornwood, NY) confocal microscope using a 63× objective (N.A. 1.4). Alignment for all three channels and resolution were checked at 8× zoom using 1 μm fluorescent spheres (Molecular Probes). The XY resolution of the instrument was ≈300 nm and all three channels were superimposed. Z-axis steps were usually 0.5 μm and the resulting images are presented as short stacks of 4–6 optical sections (2–3 μm) to compensate for slight ripples across the tissue and present an even plane of

Author Manuscript Author Manuscript Author Manuscript Author Manuscript

focus. Brightness, contrast, and color balance of digital images were adjusted in Adobe PhotoShop (San Jose, CA), but no filtering or region specific adjustments were made to any images.

Image analysis

Some digital images were analyzed with custom software that allowed the level of association between two labeled structures to be distinguished from chance (Li et al., 2002). Repeating structures of interest, such as clusters of Cx57 labeling or AT endings and B-type HC plexus, were clipped from the image by centering a sampling box on the structure. Alignment and averaging of these boxes produce a plot of color intensity versus pixel positions that reveals the spatial distribution of the immunofluorescence around a specific type of structure such as a gap junction plaque. A strong level of colocalization between two channels is revealed by two correlated peaks, whereas a caldera-like plot from one signal that is associated with a peak from another signal represents anticorrelation. A 5×5 median filter was applied for smoothing. Control images were produced by rotating one color channel out of phase, which usually produced a flat pattern without correlated peaks, representing random overlap.

RESULTS

Gene structure and sequence of rabbit Cx57

Cx57 cDNA was isolated from rabbit retina total RNA by rtPCR and Race. A total of 2.9 kb of cDNA sequence was obtained. Rabbit Cx57 cDNA contained a 1,563 basepair (bp) open reading frame that encodes a 521 aa protein with predicted molecular weight of 59 kDa (Fig. 1A). A peptide from the C-terminal, 17 residues long, was selected to generate an antibody (dashed box in Fig. 1A). The Cx57 cDNA sequence was used to BLAST search rabbit genomic sequences in GenBank (Bethesda, MD), yielding a precise match to a site in chromosome 12 (GenBank Access. No. AAGW02019415) that is annotated LOC100008928, gap junction protein alpha10. Alignment of the Cx57 cDNA sequence to the genomic sequence showed a gene structure with two exons (Fig. 1B). Note that the predicted exons annotated in LOC100008928 do not match those we have found experimentally. The entire coding region was contained within the first exon of the rabbit Cx57 gene. In contrast, for the mouse Cx57 a small fraction of the translated region was found in the second exon (Hombach et al., 2004). A neighbor-joining analysis of amino acid sequences of connexins related to mouse Cx57, with human Cx43 as an outgroup, revealed that rabbit Cx57 was most closely related to mouse Cx57 and human Cx62 (Fig. 1C). Rabbit Cx57 was distinct from human Cx59 and Cx43.

Specificity of the Cx57 antibodies in the retina

To test the specificity of the Cx57 antibodies we performed the following three experiments.

1. Hela cells were transfected with Cx57 tagged at the C-terminal with GFP according to a standard protocol. Figure 2A shows two adjacent cells with actin labeled by phalloidin. The GFP fluorescence indicates the presence of putative Cx57 gap junctions on filaments connecting adjacent cells (Fig. 2C). Double labeling shows

Author Manuscript Author Manuscript Author Manuscript Author Manuscript

that the rabbit polyclonal Cx57 antibody recognizes the same Cx57-GFP labeled structures (Fig. 2B,D). This indicates antibody specificity. However, the monoclonal Cx57 antibody did not recognize the Cx57-GFP construct.

2. A western blot of a Cx57 thioredoxin fusion protein produced a single band with the rabbit Cx57 antibody (Fig. 3). A band of the same predicted molecular weight was also stained with a thioredoxin antibody. The control lane was unstained. This experiment indicates the ability of our antibodies to recognize a Cx57 fusion protein.

3. In double-label experiments, our mouse and rabbit antibodies against Cx57 were colocalized (Fig. 4). We also compared the mouse Cx57 antibody with rabbit Cx57 antibodies obtained from Zymed (Cat. nos. 40-4800 and 40-5000) (Ciolofan et al., 2007). These were also colocalized, although the Zymed antibodies produced additional background labeling which was distributed uniformly throughout the tissue. Labeling the same structures with antibodies raised against different sequences indicates antibody specificity.

Coupling of B-type HC cells in rabbit retina

Dense labeling of A-type HCs could be produced either by intracellular dye injection or staining for calbindin (Mills and Massey, 1994; O'Brien et al., 2006). B-type HCs in the rabbit retina were targeted for intracellular dye injections by the presence of large round somas in DAPI-stained tissue (Vaney, 1991, 1993). When a B-type HC soma was filled with Neurobiotin, a large patch of coupled HCs was recovered (Fig. 5B) (Mills and Massey, 1994). The picture is dominated by well-stained somata and a dense field of overlapping somatic dendrites. At high magnification, it was observed that fine clusters of dendritic terminals contact cone pedicles (Pan and Massey, 2007). Some axons were visible leaving the periphery of the patch (not shown; Vaney, 1993) but the axon terminals were not stained by this method. Presumably, this pattern was obtained because the somatic network presented a low resistance path for the diffusion of Neurobiotin, compared with the long and narrow axons.

When the gap junctions between the HCs were blocked with meclofenamic acid (MFA; Pan et al., 2007), a completely different picture was obtained. In the absence of coupling, a single axon-bearing B-type HC was recovered (Fig. 5A). There was a nest of symmetrical dendrites around the soma but, in addition, the axon, in some cases 500 μm long, and the axon terminal were completely filled. High-resolution images show that the individual horseshoe-shaped axon terminal endings contact rod spherules (Pan and Massey, 2007). In the Cx57 knockout mouse retina, in the absence of gap junction coupling between HCs, dye injection also produced well-filled examples of single HCs with prominent axon terminals (Hombach et al., 2004; Shelley et al., 2006).

To fill the AT plexus, a slightly different procedure was followed. First, a B-type HC soma was filled with Lucifer Yellow. Because B-type HC gap junctions do not pass Lucifer Yellow (Dacheux and Raviola, 1982; Mills and Massey, 1994), a single cell with a large part of the axon became visible. Second, the axon terminal was injected with Neurobiotin at the point where the thin axon first expands. This produced a dense fill of the AT plexus, a large

Author Manuscript Author Manuscript Author Manuscript Author Manuscript

field of overlapping ATs which are independently coupled (Fig. 5C) (Pan and Massey, 2007). The absence of B-type somas and the abundance of the horseshoe-shaped terminal endings indicate that Neurobiotin was restricted to the AT plexus. In summary, by manipulating the conditions for intracellular dye injection we were able to fill the coupled network of somatic dendrites and the mosaic of B-type HC somas or the B-type AT plexus independently.

Cx57 immunoreactivity in the OPL of rabbit retina

Figure 6 shows a cross-section of the rabbit retina taken with DIC optics. Under these conditions, the different layers of the retina were clearly visible. When the sections were stained with the mouse antibody against rabbit Cx57, a single band was labeled in the OPL. The Cx57 labeling was punctate, which is consistent with the appearance of small gap junctions, and restricted to the OPL. No labeling was present in the other layers of the retina. This pattern suggests that HCs may express Cx57.

We used double- and triple-label confocal microscopy to identify reference structures in the OPL. An antibody against the metabotropic glutamate receptor mGluR6 labeled the dendritic tips of both rod bipolar cells and ON cone bipolar cells (Vardi et al., 2000; Li et al., 2004). The bright pairs show the presence of rod bipolar dendrites where they insert into single rod spherules. The clusters of finer terminals are ON cone bipolar dendrites which converge at individual cone pedicles. Several cone pedicles are marked by arrows in Figure 7A. In the rabbit retina, calbindin is a marker for HCs and their processes. Labeling with an antibody against calbindin produced dense staining of the HC processes in the OPL as well as the cell bodies protruding down into the inner nuclear layer (INL) (Fig. 7B). The brightest structures in the dense band of dendrites were contributed by A-type HCs. Slightly above the dense layer of the HC plexus, there were clusters of HC terminals at the cone pedicles previously marked for mGluR6. In addition, the calbindin antibody stained individual terminals from the ATs which arose from the plexus and wrapped around the mGluR6-labeled rod bipolar dendrites at each rod spherule. The punctate Cx57 labeling was far less numerous than the mGluR6 labeling. This suggests that, numerically, the number of rod spherules far exceeds the number of Cx57-labeled gap junctions. There was no obvious association between cone pedicles and the Cx57 labeling. Furthermore, most Cx57 clusters occurred distinctly below the level of rod spherules, yet occasionally above the cone pedicles, as previously reported (Puller et al., 2009). This suggests the Cx57 plaques may be associated with the AT plexus, which lies high in the OPL (Janssen-Bienhold et al., 2009).

To confirm these findings, we also used an antibody against RIBEYE to label synaptic ribbons in the OPL (Fig. 7C). Each rod spherule contains a single, large, horseshoe-shaped synaptic ribbon, whereas the cone pedicles contain a cluster of smaller ribbons. The mGluR6 labeled tips of rod bipolar dendrites were found nestled within each horseshoe-shaped rod synaptic ribbon. As before, the Cx57 labeling was punctate and mostly occurred below the level of rod spherules (Fig. 7D). We did not observe any Cx57 labeling specifically associated with rod spherules shown by the presence of a large synaptic ribbon. In summary, these experiments also suggest that Cx57 is expressed by HCs, but they also show there is no specific relationship between Cx57 labeling and photoreceptor terminals.

Author Manuscript Author Manuscript Author Manuscript Author Manuscript

Cx57 is not colocalized with A-type HCs

So far, we have shown that Cx57 labeling occurs in the OPL consistent with the position of HCs in the rabbit retina. However, there are three different HC networks in the OPL and it is uncertain which one(s) make use of Cx57 gap junctions. A-type HCs are extremely well coupled and the complete plexus may be stained easily by injecting several nearby A-type HCs with Neurobiotin (Pan and Massey, 2007). This material was then incubated with antibodies against Cx50 and Cx57 (Fig. 8).

We have previously shown that A-type HCs express Cx50 (O'Brien et al., 2006) and, as expected, most of the Cx50 labeling (92.5 ± 1.8%; mean ± SEM; $n = 4$) was colocalized with the dendrites of A-type HCs. To assess the probability of false-positives caused by chance overlap, we compared the original orientation of the images to those when the Cx50 channel was rotated by 90, 180, or 270°. This is sometimes known as rotational analysis. When one channel was rotated out of the original registration, the overlap fell dramatically to 13 ± 3.4% (mean ± SEM; $n = 4$) (Fig. 9A). A large reduction is the signature of true colocalization in the original and this was confirmed by the labeling pattern whereby many of the Cx50 plaques occurred at dendritic crossings in the A-type plexus.

In contrast, Cx57 labeling did not occur on the A-type HCs. Less than 4.5 ± 1.8% (mean ± SEM; $n = 4$) of the Cx57 labeling was colocalized with the plexus of A-type HCs. Although this is close to zero, the small remnant may be due to the relatively low Z-axis resolution or minor errors in colocalization. When one channel from this image was rotated out of alignment, the apparent overlap of Cx57 actually increased to 14 ± 3.9% (mean ± SEM; $n = 4$) (Fig. 9B). This indicates that the Cx57 labeling is anticorrelated with A-type HCs or, in other words, Cx57 plaques avoid A-type HCs. In addition, it should be noted there was practically no colocalization between Cx50 and Cx57, which further suggests they represent different gap junctions on distinct cell types. Finally, there were no giant plaques among the Cx57 population.

Cx57 is not colocalized with the somatic dendrites of B-type HC

We have shown that Cx57 labeling occurs in the OPL, in a position consistent with HC labeling, yet Cx57 labeling is not colocalized with A-type HCs. Therefore, we stained the plexus of somatic dendrites belonging to B-type HCs via tracer injection and examined the colocalization with Cx57. Figure 10A shows a confocal stack from a patch of B-type HC somas and somatic dendrites. The cell bodies were proximal to the dendritic plexus and the stack was 6.6 μm thick (23 × 0.3 μm sections), from the somas to the dendritic clusters that invaginate cone pedicles. It is important to note that there were none of the characteristic AT endings in this field, which indicates the absence of AT processes. In other words, the Neurobiotin labeling in Figure 10A was restricted to B-type somas and somatic dendrites.

In double-label experiments, a full-thickness stack can produce false-positive results. Therefore, we took two mini-stacks (0.9 μm thick, 3 × 0.3 μm sections), one through the somas and major dendrites and one more distal, close to the level of the cone pedicles. At the level of the B-type somatic dendrites, there was very little Cx57 labeling and it did not occur on the major dendrites of B-type HCs (Fig. 10B). Higher in the OPL, the cell bodies

Author Manuscript Author Manuscript Author Manuscript Author Manuscript

were mostly out of focus, the dendrites were finer, and the terminal clusters were more prominent, marking the sites of individual cone pedicles (arrows in Fig. 10C). At this level, high in the OPL, there was much more Cx57 labeling but it was not colocalized with the somatic plexus of B-type HCs. It is important to note there was no obvious association between Cx57 plaques and the terminal clusters that indicate cone contacts. The Cx57 plaques appear magenta, as opposed to white, because they were not on the somatic dendrites of B-type HCs. In fact, the OPL is partially stratified such that the major dendrites of A-type HCs run at the bottom, adjacent to the INL, while the B-type HC plexus is slightly higher (Pan and Massey, 2007). The AT network is still more distal, adjacent to the photoreceptor terminals. Therefore, the location of most Cx57 plaques, high in the OPL, suggests an association with the AT plexus, as also reported for Cx57 in the mouse retina (Janssen-Bienhold et al., 2009).

We performed a quantitative analysis of colocalization for Cx57 and the somatic dendrites of B-type HCs using single confocal sections. In the original orientation, only 6.7 ± 4.2% (mean ± SEM; $n = 4$) of the Cx57 pixels were colocalized with the somatic dendrites of B-type HCs. Again, this is close to zero, but the small remnant may be due to the limitations of Z-axis resolution and the colocalization routines. Interestingly, when one channel of the image was rotated, thus destroying the spatial organization of the original, the fraction of colocalized Cx57 plaques rose to 15.5 ± 5.6% (mean ± SEM; $n = 4$) (Fig. 9C). In other words, randomly rotating one channel caused an increase in the probability of colocalization. This indicates that, in the original image, the Cx57 plaques, actually avoided the somatic dendrites. Thus, the Cx57 labeling was anticorrelated with the network of B-type somatic dendrites.

We also analyzed this material with signal-averaging colocalization software. A sampling box was centered over every Cx57 plaque and these segments were aligned and averaged. When the results were plotted as a 3D graph with pixel intensity on the z-axis, there was a sharp peak of Cx57 immunolabeling surrounded by a plain of low noise (Fig. 11A). There was no corresponding peak in the channel showing the somatic dendrites of B-type HCs. In fact, this channel had a low point, less than the background signal, coincident with the Cx57 peak (Fig. 11B). This analysis, which shows the average distribution of B-type dendrites around a Cx57 plaque, also indicates that Cx57 labeling was not associated with the somatic dendrites of B-type HCs.

Cx57 is colocalized with the B-type axon terminal plexus

In similar experiments, the AT plexus was labeled after filling with Neurobiotin. It should be noted that there were no B-type somas in this frame, but the typical horseshoe-shaped AT endings were abundant, with a distribution to match the rod density. This indicates that Neurobiotin labeling was restricted to the AT plexus and there are no somatic dendrites in this frame (Fig. 12A). In this material, it was immediately obvious that most of the Cx57 plaques appeared yellow because they were colocalized with the AT plexus (Fig. 12B). At higher magnification, the AT endings were prominent and some individual terminals were visible. The Cx57 plaques occurred on the AT processes, many at the intersection sites of multiple processes, or between processes that were cofasciculated (Fig. 12C,D). However,

Author Manuscript Author Manuscript Author Manuscript Author Manuscript

the density and complexity of the AT plexus made it difficult to resolve individual terminal crossings. Cx57 plaques were not located at the fine AT endings that contacted individual rod spherules. Rather, the Cx57 was restricted to the AT plexus.

Quantitative analysis of this material revealed that 96.9 ± 2.6% (mean ± SEM; $n = 4$) of the Cx57 labeling was colocalized with the AT plexus. When one channel was rotated out of alignment, the apparent colocalization was reduced to 16 ± 9.8% (mean ± SEM; $n = 4$; Fig. 9D). The ratio of the original to the rotated images indicates that in the original image the colocalization of Cx57 with the AT plexus was far greater than random overlap. It is important to note that the colocalization was almost complete in the original image, but it was dramatically reduced by the rotation of one channel. In contrast, the apparent overlap of Cx57 with the somatic dendrites of B-type HCs was increased by rotation (Fig. 9C). This analysis strongly suggests that Cx57 is colocalized with the axon terminal plexus.

When this material was analyzed with our colocalization software, there was a pronounced peak in the AT channel corresponding to the peak in the Cx57 channel (Fig. 11C,D). This indicates that there is a high probability that an AT process will be found at the location of each Cx57 plaque. This stands in contrast to the results for the somatic dendrites of B-type HCs, which are anticorrelated with Cx57 labeling. As above, we conclude that Cx57 is colocalized with the AT plexus.

Comparison between Cx57 and Cx50

In double-label material, it is interesting to compare the Cx57 gap junctions on the AT plexus with the Cx50 gap junctions of A-type HCs. The Cx57 plaques were more numerous but uniformly small in size compared with the Cx50 plaques. Most Cx57 plaques fell in the range from 0.3 μm to 1 μm in diameter, 0.1 μm^2 to 1 μm^2. The mean diameter of the Cx57 plaques was 0.56 ± 0.01 μm (mean ± SEM, $n = 580$), or 0.27 ± 0.01 μm^2 (mean ± SEM, $n = 580$) in area. The largest Cx57 plaque we observed was ≈1.7 μm in diameter but this was rare. In contrast, the Cx50 plaques had a mean diameter of 1.07 ± 0.05 μm (mean ± SEM, $n = 295$) or 1.40 ± 0.19 μm^2 (mean ± SEM, $n = 295$) in area. There were giant plaques, up to 36 μm^2, in the Cx50 material as well as many small plaques less than 1 μm^2 in diameter. Thus, there was much greater variation in the Cx50 population (range, 0.06–36 μm^2) while the Cx57 plaques fell in a narrow size range (0.06–1.6 μm^2). The uniform size of the Cx57 gap junctions may be a consequence of the fine, relatively consistent structure of the axon terminals. In contrast, the massive primary dendrites of A-type HCs, especially those close to the soma, present opportunities for substantial overlap. These are the sites of giant gap junction plaques that contribute to the extensive coupling of the A-type HC plexus. Giant plaques of this description are entirely absent in the Cx57 material.

The Cx57/Cx50 double-label experiments clearly show that the two sets of gap junctions are completely independent. However, this material also presents an opportunity to compare the total area of gap junctions for each connexin type. The total pixel area for Cx50 was greater by a ratio of ≈3:2. In superior retina, we estimated that the area of Cx50 plaques was 2.5×10^4 $\mu m^2/mm^2$ compared with 1.7×10^4 $\mu m^2/mm^2$ for Cx57. Dividing by the cell density in superior retina for A-type HCs, 200/mm^2 (Mills and Massey, 1994), gives 125 μm^2 of Cx50 gap junction per A-type HC, comparable to previously published results (O'Brien et al.,

Author Manuscript Author Manuscript Author Manuscript Author Manuscript

2006). By comparison, dividing by the B-type HC density, 400/mm^2 (Mills and Massey, 1994), we estimated a total of 41.25 μm^2 of Cx57-labeled gap junction per AT. Thus, in terms of gap junctional area alone, it can be seen that A-type HCs are better coupled than ATs by a factor of ≈3. In fact, this is an underestimation of the relative coupling in A-type HCs versus ATs because other factors such as coverage, the unitary conductance, and the gating properties of the respective connexins must also be taken into account (see below).

Electron microscopy for Cx57

The monoclonal Cx57 antibody was also suitable for preembedding immunolabeling and electron microscopy. In Figure 13, a row of rod spherules, marked by prominent synaptic ribbons, can be seen at the top of the frame. Each rod spherule is packed with synaptic vesicles and, depending on the section plane, the postsynaptic invagination occurs close to the synaptic ribbon. Below the level of rod spherules, in the OPL, we found small deposits of Cx57-like immunoreactivity between adjacent processes. As shown here, the Cx57-like immunoreactivity invaginated the larger process. The size of these potential Cx57 gap junctions was relatively uniform and we never observed giant plaques of the type described for Cx50 in A-type HCs. The labeling was present along the cell membranes but the classical pentilaminar appearance of gap junctions was not apparent, probably due to the limitations imposed by immunoelectron microscopy. Invaginating gap junctions of this description have been described previously in other tissues (Raviola et al., 1980). It is not possible to identify the Cx57-labeled processes, but by their position high in the OPL they are most likely AT processes. This putative Cx57-labeled gap junction, between two fasciculated terminals, is consistent with Cx57 labeling of the AT plexus. Finally, we never observed Cx57-like immunoreactivity associated either with rod spherules or cone pedicles.

DISCUSSION

By combining intracellular dye injections with immunofluorescence, we examined the distribution of Cx57 in the rabbit retina. Our major findings may be summarized as follows: We confirmed previous reports that Cx57 is restricted to HCs in the OPL (Puller et al., 2009). Intracellular dye injection indicates there are three independently coupled networks of HC processes in the OPL, as previously reported (Vaney, 1993). Cx57 is strongly colocalized with the B-type axon terminal plexus but not with the somatic dendrites of A- or B-type HCs. This shows that multiple neuronal connexins are expressed in the retina and that different coupled HC networks use distinct connexins.

Antibody specificity

The results presented here are critically dependent on the specificity of the antibodies employed. For the well-known antibodies used to label reference structures such as synaptic ribbons, synaptic vesicles, and glutamate receptors, there are many examples from the literature that provide a high level of confidence. The Cx57 antibodies developed for this project require more specific tests to establish specificity. Three different tests were used to validate the use of Cx57 antibodies.

Author Manuscript Author Manuscript Author Manuscript Author Manuscript

First, we transfected HeLa cells with Cx57-GFP, which was expressed in gap junctions between neighboring cells anchored by actin filaments as shown by the presence of GFP fluorescence (Fig. 2). These same punctate gap junctions were also recognized by the rabbit polyclonal Cx57 antibody. Second, we constructed a thioredoxin fusion protein. A band at the same molecular weight was recognized by both thioredoxin antibodies and the Cx57 antibody (Fig. 3). Third, in double-label studies the monoclonal mouse antibody was colocalized with the polyclonal rabbit antibody (Fig. 4A–C).

The monoclonal Cx57 antibody was also colocalized with commercially available Cx57 antibodies from Zymed raised in rabbit. In these experiments, there were many double-labeled plaques that were taken as Cx57 plaques. In addition, there were many single-labeled puncta stained only by the Zymed antibodies. These were smaller than the double-labeled plaques with a random distribution not associated with any of the HC types. Furthermore, the single-labeled profiles were present throughout the retina, including the inner retina. This region contains no HC processes and no Cx57 gap junctions. We ascribe this pattern to nonspecific background labeling from the Zymed antibodies. In addition, we note that one of the Zymed antibodies (Zymed 40-4800) produced nonspecific labeling in the Cx57 knockout mouse (Ciolofan et al., 2007).

Unique association of Cx57 with the B-type HC axon terminal plexus

Simple inspection suggested that most Cx57 plaques were colocalized with the AT plexus (Fig. 12) and most Cx50 plaques were colocalized with the A-type HC plexus (Fig. 8). Very few gap junctions of either type were associated with the somatic dendrites of B-type HCs. It was important to compare the labeling patterns for each connexin/HC type and to analyze this material in a quantitative manner to determine if there were sufficient gap junctions to account for coupling in all networks. Colocalization was assessed on a pixel basis or by counting individual Cx50 or Cx57 plaques in all three HC networks. To assess the probability of false-positives caused by chance overlap, we compared the original orientation of the images to those when the Cx57 channel was rotated by 90, 180, or 270° (Fig. 9).

For Cx50/A-type HC and Cx57/AT, the rotational analysis produced the same profile. In the original orientation the colocalization was dramatically higher than for any of the rotated images. All three rotated control orientations gave comparably poor results. This profile, with a ratio >6 for the original/mean of the rotated images, is the signature for colocalization in the original (Fig. 9A,D). In contrast, Cx57/A-type HC and Cx57/B-type HC both produced the opposite profile whereby the apparent colocalization in the rotated images was greater than the original with a ratio of < 0.5 (Fig. 9B,C). In other words, the apparent colocalization in the original images was actually less than expected by random chance. The ratio of the original/mean of the rotated images for Cx57/A-type HC was 0.32 and for Cx57/B-type HC it was 0.43. This profile is consistent with anticorrelation and provides evidence against colocalization for Cx57/A-type HC and Cx57/B-type HC. In other words, the somatic dendrites of B-type HCs were not labeled for Cx57 or Cx50 and neither connexin can account for coupling in this network. In turn, this may suggest the presence of an unidentified connexin in B-type HCs.

Author Manuscript Author Manuscript Author Manuscript Author Manuscript

HC gap junctions

In the rabbit retina, A-type HCs, B-type HCs, and B-type ATs have distinctly different properties. Lucifer Yellow passes through A-type HC gap junctions but not through those of B-type HCs or B-type ATs (Vaney, 1993). This immediately suggests that A-type HCs express a distinct connexin, which has previously been identified as Cx50. The present results suggest that Cx57 is colocalized with the AT plexus but the connexin expressed by the somatic dendrites of B-type HCs is unknown.

Previous studies of both dye coupling and receptive field measurements have shown that gap junction coupling in rabbit HCs follows the order: A-type ≫ B-type > AT (Dacheux and Raviola, 1982; Bloomfield et al., 1995). If coupling in the somatic dendrites of B-type HCs exceeds coupling in B-type ATs, yet both were due to the expression of Cx57, we should expect more Cx57 gap junctions on the somatic dendrites. In fact, we find the opposite result: 95% of the Cx57 labeling was associated with the AT plexus and only a small fraction, ≈5%, was colocalized with the somatic dendrites of B-type HCs. Even this 5% is close enough to zero to fall within the limits of experimental error. This is somewhat consistent with the distribution of Cx57 in the mouse retina where the axon terminals expressed more Cx57 than the somatic dendrites (Janssen-Bienhold et al., 2009). However, even 5% is less than expected from random chance overlap. This small fraction is certainly not enough to account for the greater coupling of the somatic dendrites of B-type HCs. There are two independently coupled networks in B-type HCs. Therefore, we propose that another unidentified connexin is expressed by B-type HCs. We also note that in the Cx57 knockout mouse, some somatic HC coupling remained, perhaps also suggesting the presence of an additional gap junction protein in mouse axon-bearing HCs (Shelley et al., 2006).

On a note of caution, we are unable to rule out that our Cx57 antibody does not recognize the form of Cx57 expressed by the somatic dendrites of B-type HCs. Examples of posttranslational modification may include phosphorylation or acetylation, among other possibilities (Locke et al., 2009). Phosphorylation, under the control of specific kinases, has been reported as a mechanism to control the conductance of Cx36 gap junctions (Kothmann et al., 2007). The peptide sequence used to produce antibodies against rabbit Cx57 contains three serine residues that are potential phosphorylation sites. Conceivably, phosphorylation at one of these sites could interfere with antibody recognition so that B-type HCs appear unlabeled for Cx57. However, the two Zymed antibodies, raised against different sequences in the C-terminal of Cx57, also failed to recognize the somatic dendrites of B-type HCs. This makes it less likely that biochemical modification of Cx57 prevents antibody recognition unless there is a major truncation of the C-terminal. It would be informative to compare labeling with an antibody raised against the intracellular loop. However, our attempts to raise antibodies against this region were not effective.

Relative coupling in HC networks

Considering the dramatic difference in receptive field measurements, A-type HC ≫ B-type HC > B-type AT (Dacheux and Raviola, 1982; Bloomfield et al., 1995), our calculations of the total area of gap junctions were surprisingly comparable for Cx50 and Cx57 gap junctions. The gap junction area of Cx50/A-type HC was three times greater than Cx57/AT.

Author Manuscript Author Manuscript Author Manuscript Author Manuscript

Yet the diffusion coefficient for dye transfer in A-type HCs was greater than B-type HCs by a factor of 20 (Mills and Massey, 1998) and the ratio must be even greater for A-type HCs compared with ATs. This suggests that most of the difference between A-type HCs and B-type ATs may be due to the large difference in the unitary conductance of their respective gap junction channels.

The factors affecting cell coupling may be summarized as the product of plaque size, unitary conductance, and the channel gating properties of each gap junction type. For both Cx50 and Cx57 gap junctions the gating properties are unknown. However, it has been estimated that a small fraction of gap junction channels, ≈1%, are open at any one time (Bukauskas et al., 2000) and we presume these numbers are comparable for Cx50 and Cx57 channels. However, the unitary conductance of Cx50 is 220pS compared with 52pS for Cx57 and this may account for a large part of the difference between the two networks. If 1% of the channels are open, then in 125 μm^2/A-type HC there are $\approx 1.25 \times 10^4$ open Cx50 channels yielding a network conductance of 2.75 μS. For 41 μm^2/AT, there are $\approx 4.1 \times 10^3$ open Cx57 channels yielding a network conductance of 0.21 μS. Dividing by the coverage in superior retina, six for A-type HCs and 10 for ATs (Mills and Massey, 1994; Pan and Massey, 2007), we obtain ≈2 MΩ of transjunctional resistance between two neighboring A-type HCs compared with 43 MΩ for two ATs. These calculations, although necessarily approximate, suggest that A-type HCs are better coupled than ATs by a factor of ≈20. In round numbers, the ratio is accounted for by a factor of ≈4 in unitary conductance, ≈3 in the density of gap junctions, and ≈2 in coverage for Cx50/A-type HC compared with Cx57/B-type AT. Thus, the ratio is dominated by the difference in unitary conductance between Cx50 and Cx57. In turn, this suggests that different neuronal types express distinct connexins in order to provide specific properties for the resulting network. It is also possible that the expression of distinct connexins in the HCs may provide the opportunity for differential modulation under varying light conditions.

Cx57 in the mouse retina

The original work with Cx57 made use of the mouse retina because of the availability of a lacZ reporter and Cx57 knockout mice. Cx57 labeling was restricted to the OPL, which is consistent with expression by HCs (Hombach et al., 2004; Ciolofan et al., 2007; Kihara et al., 2008). Furthermore, in the Cx57 knockout mouse, dye coupling in HCs was dramatically reduced and the axon terminals became visible. However, some HC coupling was still observed in the Cx57 knockout mouse (Shelley et al., 2006) and this may indicate that a second connexin is expressed in mouse HCs, as reported for zebrafish retina (Shields et al., 2007). The axon terminal staining indicates reduced coupling between the somatic dendrites; the axon terminal labeling occurred because of the reduced network coupling, similar to the results obtained in the rabbit retina when B-type HC gap junctions were blocked with an antagonist (Pan et al., 2007). Finally, in the Cx57 knockout mouse the size of the receptive field was also reduced, consistent with the lack of gap junction coupling (Shelley et al., 2006). In summary, these studies indicate that mouse HCs are coupled via Cx57 gap junctions but they did not address the coupling of the AT network. Most recently, Janssen-Bienhold et al. (2009) showed that Cx57 labeling was present in both the dendrites and axon terminal processes of isolated mouse HCs. In addition, more Cx57 plaques were found in the

Author Manuscript Author Manuscript Author Manuscript Author Manuscript

distal OPL and this is consistent with labeling of the mouse ATs (Janssen-Bienhold et al., 2009), similar to the pattern reported here for the rabbit retina.

Due to the limitations of calbindin as an HC marker and the difficulty of dye injecting HCs in the mouse retina, it was not possible to show Cx57 antibody labeling of HC dendrites or ATs in wholemount retina. In fact, the double-label studies of Cx57 and calbindin-labeled mouse HCs show poor or incomplete colocalization (Kihara et al., 2008). In the absence of reliable HC markers, reference structures such as synaptic ribbons were stained and some Cx57 labeling was observed within the rod spherule in close proximity to the synaptic ribbon (Ciolofan et al., 2007). We were unable to confirm this result in either mouse or rabbit retina using the antibody raised against rabbit Cx57 or the commercially available antibodies against mouse Cx57. Furthermore, other groups reported no association between Cx57 plaques and rod spherules in mouse retina (Janssen-Bienhold et al., 2009; Puller et al., 2009).

Hemichannel-mediated feedback

The mechanism of HC feedback is unknown. However, an ephaptic mechanism utilizing hemichannel-mediated feedback has been proposed (Kamermans and Spekreijse, 1999). The present results do not support a role for Cx57 in hemichannel-mediated feedback. First, the Cx57 plaques were always lower than the photoreceptor terminals, embedded in the HC plexus, and, second, in wholemount preparations, we found no pattern between Cx57 plaques and cone pedicles or rod spherules. It should be noted that these results do not rule out the participation of hemichannels constructed from a different connexin, and multiple connexins have been reported in HCs of the zebrafish retina (Shields et al., 2007). A similar conclusion was reached concerning Cx57 in the mouse retina (Janssen-Bienhold et al., 2009).

Acknowledgments

National Eye Institute (NEI); Grant numbers: EY 06515 (to S.C.M.), EY 10121 (to S.L.M.), EY 12857 (to J.O.B.), and EY 10608 (Vision Core Grant); Grant sponsor: Research to Prevent Blindness to the Department of Ophthalmology and Visual Science; S.C.M. is the Elizabeth Morford Professor of Ophthalmology and Visual Science.

LITERATURE CITED

Bloomfield SA, Xin D, Persky SE. A comparison of receptive field and tracer coupling size of horizontal cells in the rabbit retina. Vis Neurosci. 1995; 12:985–999. [PubMed: 8924420]

Bukauskas FF, Jordan K, Bukauskiene A, Bennett MV, Lampe PD, Laird DW, Verselis VK. Clustering of connexin 43-enhanced green fluorescent protein gap junction channels and functional coupling in living cells. Proc Natl Acad Sci U S A. 2000; 97:2556–2561. [PubMed: 10706639]

Ciolofan C, Lynn BD, Wellershaus K, Willecke K, Nagy JI. Spatial relationships of connexin36, connexin57 and zonula occludens-1 in the outer plexiform layer of mouse retina. Neuroscience. 2007; 148:473–488. [PubMed: 17681699]

Connors BW, Long MA. Electrical synapses in the mammalian brain. Annu Rev Neurosci. 2004; 27:393–418. [PubMed: 15217338]

Dacheux RF, Raviola E. Horizontal cells in the retina of the rabbit. J Neurosci. 1982; 2:1486–1493. [PubMed: 6181232]

Author Manuscript Author Manuscript Author Manuscript Author Manuscript

Deans MR, Volgyi B, Goodenough DA, Bloomfield SA, Paul DL. Connexin36 is essential for transmission of rod-mediated visual signals in the mammalian retina. Neuron. 2002; 36:703–712. [PubMed: 12441058]

Felsenstein, J. PHYLIP (Phylogeny Inference Package). Version 3.57c: distributed by the author. 1995.

Goodenough DA, Paul DL. Beyond the gap: functions of unpaired connexon channels. Nat Rev Mol Cell Biol. 2003; 4:285–294. [PubMed: 12671651]

Hombach S, Janssen-Bienhold U, Sohl G, Schubert T, Bussow H, Ott T, Weiler R, Willecke K. Functional expression of connexin57 in horizontal cells of the mouse retina. Eur J Neurosci. 2004; 19:2633–2640. [PubMed: 15147297]

Janssen-Bienhold U, Trumpler J, Hilgen G, Schultz K, Muller LP, Sonntag S, Dedek K, Dirks P, Willecke K, Weiler R. Connexin57 is expressed in dendro-dendritic and axo-axonal gap junctions of mouse horizontal cells and its distribution is modulated by light. J Comp Neurol. 2009; 513:363–374. [PubMed: 19177557]

Kamermans M, Spekreijse H. The feedback pathway from horizontal cells to cones. A mini review with a look ahead. Vision Res. 1999; 39:2449–2468. [PubMed: 10396615]

Kihara AH, Santos TO, Paschon V, Matos RJ, Britto LR. Lack of photoreceptor signaling alters the expression of specific synaptic proteins in the retina. Neuroscience. 2008; 151:995–1005. [PubMed: 18248909]

Kothmann WW, Li X, Burr GS, O'Brien J. Connexin 35/36 is phosphorylated at regulatory sites in the retina. Vis Neurosci. 2007; 24:363–375. [PubMed: 17640446]

Li W, Trexler EB, Massey SC. Glutamate receptors at rod bipolar ribbon synapses in the rabbit retina. J Comp Neurol. 2002; 448:230–248. [PubMed: 12115706]

Li W, Keung JW, Massey SC. Direct synaptic connections between rods and OFF cone bipolar cells in the rabbit retina. J Comp Neurol. 2004; 474:1–12. [PubMed: 15156575]

Locke D, Bian S, Li H, Harris AL. Post-translational modifications of connexin26 revealed by mass spectrometry. Biochem J. 2009; 424:385–398. [PubMed: 19775242]

Masland RH. The fundamental plan of the retina. Nat Neurosci. 2001; 4:877–886. [PubMed: 11528418]

Massey SC, Mills SL. A calbindin-immunoreactive cone bipolar cell type in the rabbit retina. J Comp Neurol. 1996; 366:15–33. [PubMed: 8866843]

Massey SC, Mills SL. Gap junctions between AII ama-crine cells and calbindin-positive bipolar cells in the rabbit retina. Vis Neurosci. 1999; 16:1181–1189. [PubMed: 10614597]

Menichella DM, Goodenough DA, Sirkowski E, Scherer SS, Paul DL. Connexins are critical for normal myelination in the CNS. J Neurosci. 2003; 23:5963–5973. [PubMed: 12843301]

Mills SL, Massey SC. Distribution and coverage of A-and B-type horizontal cells stained with Neurobiotin in the rabbit retina. Vis Neurosci. 1994; 11:549–560. [PubMed: 7518689]

Mills SL, Massey SC. The kinetics of tracer movement through homologous gap junctions in the rabbit retina. Vis Neurosci. 1998; 15:765–777. [PubMed: 9682877]

Mills SL, Massey SC. A series of biotinylated tracers distinguishes three types of gap junction in retina. J Neurosci. 2000; 20:8629–8636. [PubMed: 11069972]

Nelson R, von Litzow A, Kolb H, Gouras P. Horizontal cells in cat retina with independent dendritic systems. Science. 1975; 189:137–139. [PubMed: 1138370]

O'Brien JJ, Li W, Pan F, Keung J, O'Brien J, Massey SC. Coupling between A-type horizontal cells is mediated by connexin 50 gap junctions in the rabbit retina. J Neurosci. 2006; 26:11624–11636. [PubMed: 17093084]

Palacios-Prado N, Sonntag S, Skeberdis VA, Willecke K, Bukauskas FF. Gating, permselectivity and pH-dependent modulation of channels formed by connexin57, a major connexin of horizontal cells in the mouse retina. J Physiol. 2009; 587(Pt 13):3251–3269. [PubMed: 19433576]

Pan F, Massey SC. Rod and cone input to horizontal cells in the rabbit retina. J Comp Neurol. 2007; 500:815–831. [PubMed: 17177254]

Pan F, Mills SL, Massey SC. Screening of gap junction antagonists on dye coupling in the rabbit retina. Vis Neurosci. 2007; 24:609–618. [PubMed: 17711600]

Author Manuscript Author Manuscript Author Manuscript Author Manuscript

Pandarinath C, Bomash I, Victor JD, Prusky GT, Tschetter WW, Nirenberg S. A novel mechanism for switching a neural system from one state to another. Front Comput Neurosci. 2010; 4:2. [PubMed: 20407612]

Peichl L, Gonzalez-Soriano J. Morphological types of horizontal cell in rodent retinae: a comparison of rat, mouse, gerbil, and guinea pig. Vis Neurosci. 1994; 11:501–517. [PubMed: 8038125]

Puller C, de Sevilla Muller LP, Janssen-Bienhold U, Haverkamp S. ZO-1 and the spatial organization of gap junctions and glutamate receptors in the outer plexiform layer of the mammalian retina. J Neurosci. 2009; 29:6266–6275. [PubMed: 19439604]

Raviola E, Goodenough DA, Raviola G. Structure of rapidly frozen gap junctions. J Cell Biol. 1980; 87:273–279. [PubMed: 7419595]

Schmitz F, Konigstorfer A, Sudhof TC. RIBEYE, a component of synaptic ribbons: a protein's journey through evolution provides insight into synaptic ribbon function. Neuron. 2000; 28:857–872. [PubMed: 11163272]

Semple-Rowland SL, L P, Bronson JD, Nykamp K, Streit WJ, Baehr W. Characterization of the chicken GCAP gene array and analyses of GCAP1, GCAP2, and GC1 gene expression in normal and rd chicken pineal. Mol Vis. 1999; 5:14. [PubMed: 10427104]

Shelley J, Dedek K, Schubert T, Feigenspan A, Schultz K, Hombach S, Willecke K, Weiler R. Horizontal cell receptive fields are reduced in connexin57-deficient mice. Eur J Neurosci. 2006; 23:3176–3186. [PubMed: 16820008]

Shields CR, Klooster J, Claassen Y, Ul-Hussain M, Zoidl G, Der-mietzel R, Kamermans M. Retinal horizontal cell-specific promoter activity and protein expression of zebrafish connexin 52.6 and connexin 55.5. J Comp Neurol. 2007; 501:765–779. [PubMed: 17299759]

tom Dieck S, Altrock WD, Kessels MM, Qualmann B, Regus H, Brauner D, Fejtova A, Bracko O, Gundelfinger ED, Brandstatter JH. Molecular dissection of the photoreceptor ribbon synapse: physical interaction of Bassoon and RIBEYE is essential for the assembly of the ribbon complex. J Cell Biol. 2005; 168:825–836. [PubMed: 15728193]

Vaney DI. Many diverse types of retinal neurons show tracer coupling when injected with biocytin or Neurobiotin. Neurosci Lett. 1991; 125:187–190. [PubMed: 1715532]

Vaney DI. The coupling pattern of axon-bearing horizontal cells in the mammalian retina. Proc R Soc Lond Ser B Biol Sci. 1993; 252:93–101.

Vaney DI, Weiler R. Gap junctions in the eye: evidence for heteromeric, heterotypic and mixed-homotypic interactions. Brain Res Brain Res Rev. 2000; 32:115–120. [PubMed: 10751660]

Vardi N, Duvoisin R, Wu G, Sterling P. Localization of mGluR6 to dendrites of ON bipolar cells in primate retina. J Comp Neurol. 2000; 423:402–412. [PubMed: 10870081]

Willecke K, Eiberger J, Degen J, Eckardt D, Romualdi A, Gulde-nagel M, Deutsch U, Sohl G. Structural and functional diversity of connexin genes in the mouse and human genome. Biol Chem. 2002; 383:725–737. [PubMed: 12108537]

Zappala A, Parenti R, La Delia F, Cicirata V, Cicirata F. Expression of connexin57 in mouse development and in harmaline-tremor model. Neuroscience. 2010; 171:1–11. [PubMed: 20849935]

Zhang C. Expression of connexin 57 in the olfactory epithelium and olfactory bulb. Neurosci Res. 2011; 71:226–234. [PubMed: 21840349]

Author Manuscript Author Manuscript Author Manuscript Author Manuscript

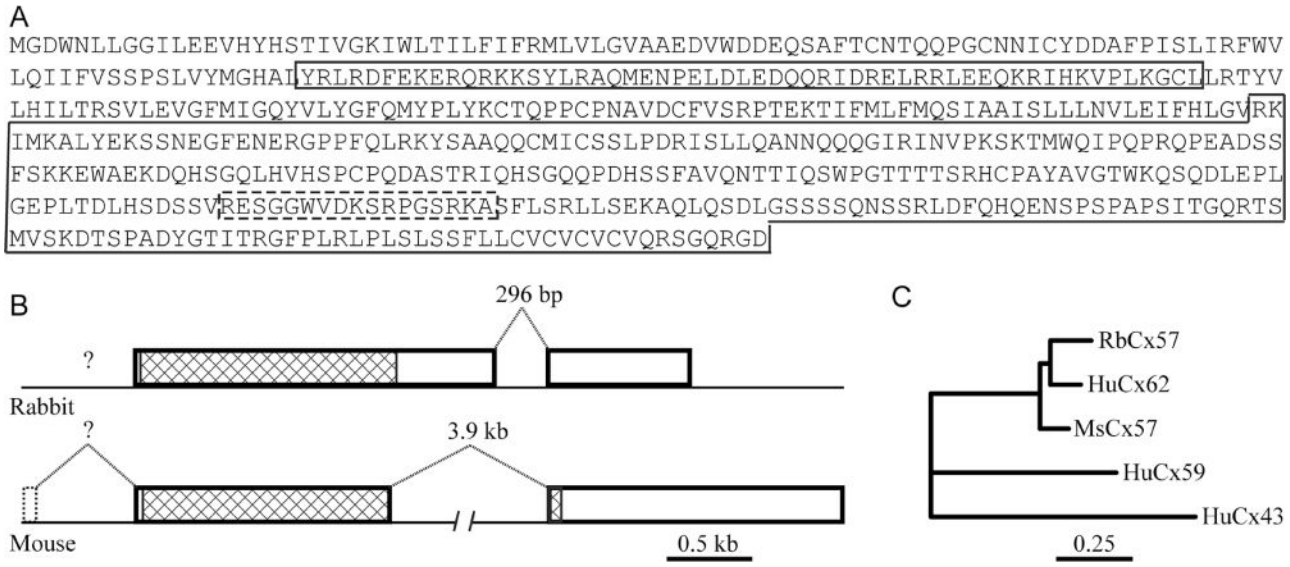

Figure 1.

Gene structure for Cx57. **A**: The sequence of rabbit Cx57. The intracellular loop is in the first small box and the C-terminal is in the second large box. The antibody epitope is indicated by a dashed box. **B**: Gene structure of rabbit Cx57 compared with mouse Cx57. The open reading frame for rabbit Cx57 is enclosed in exon 1. **C**: Dendrogram showing the neighbor-joining analysis of amino acid sequences for rabbit Cx57 and close relatives. The rabbit Cx57 sequence is most closely related to human Cx62 and mouse Cx57 and distinct from human Cx59 and Cx43.

Author Manuscript Author Manuscript Author Manuscript Author Manuscript

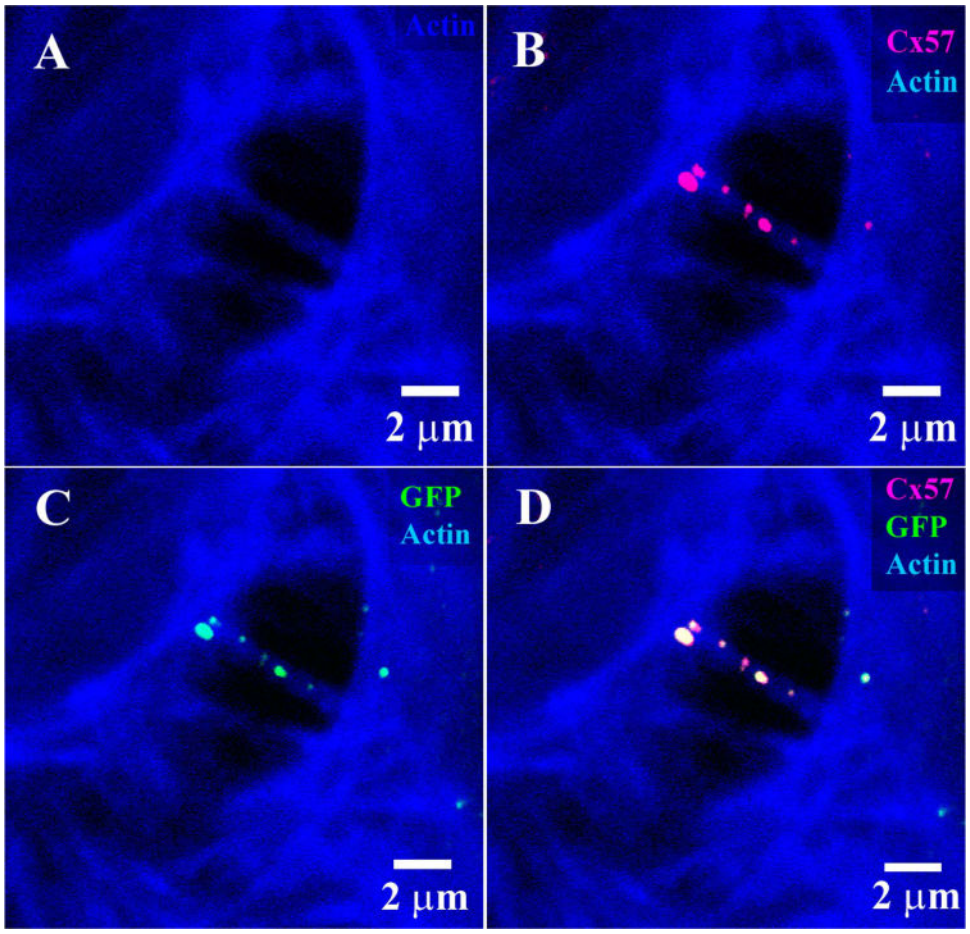

Figure 2.

Cx57 labeling of Cx57-GFP transfected cells. **A**: two adjacent Hela cells with processes that contain actin filaments, labeled with Alexa Fluor 633 phalloidin (blue). **B**: The same field stained with rabbit polyclonal Cx57 antibody (magenta). **C**: Cx57-GFP plaques were located along the connecting filaments. **D**: Double label showing colocalization of the Cx57 antibody with Cx57-GFP. This indicates specificity of the rabbit Cx57 antibody.

Author Manuscript Author Manuscript Author Manuscript Author Manuscript

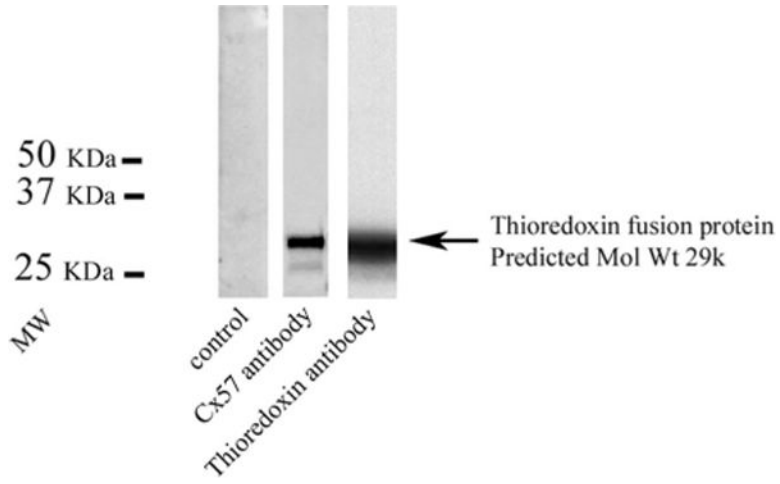

Figure 3.

Western blot, Cx57 fusion protein. Lane 1, control, no staining, lane 2, rabbit Cx57 staining of a thioredoxin fusion protein, lane 3, same molecular weight band stained with a thioredoxin antibody. This shows that the rabbit Cx57 antibody recognizes a Cx57 fusion protein.

Author Manuscript Author Manuscript Author Manuscript Author Manuscript

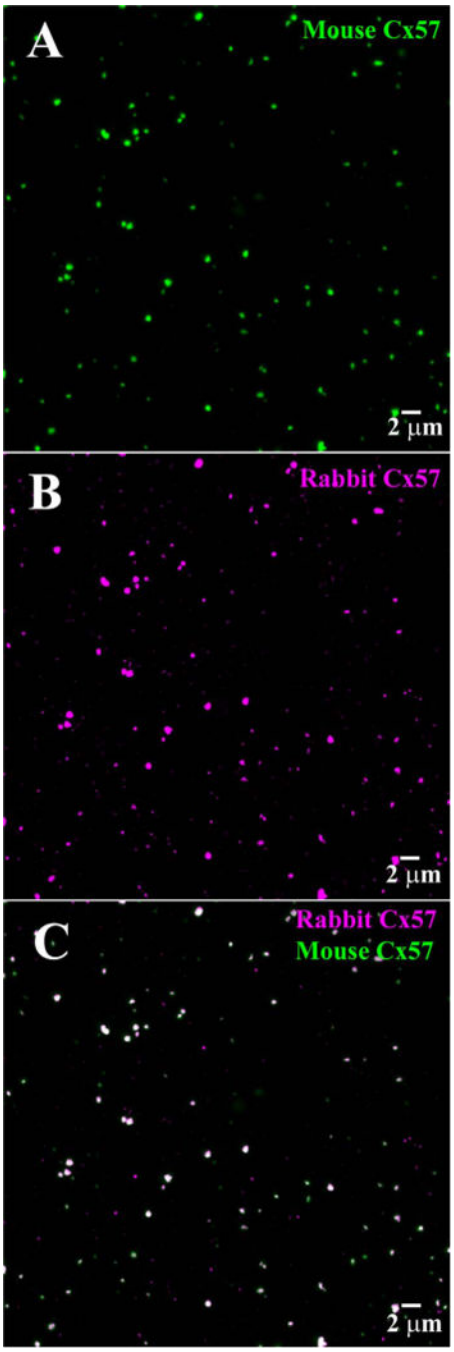

Figure 4.

A comparison of rabbit polyclonal and mouse monoclonal Cx57 antibodies. **A**: Wholemount rabbit retina, focus at the OPL, many Cx57 plaques were labeled with the mouse Cx57 antibody. **B**: Same field, many of the same Cx57 plaques were labeled with the rabbit Cx57 antibody. **C**: Double label showing almost complete colocalization for the two antibodies. This indicates the mouse and rabbit Cx57 antibodies label the same target.

Author Manuscript Author Manuscript Author Manuscript Author Manuscript

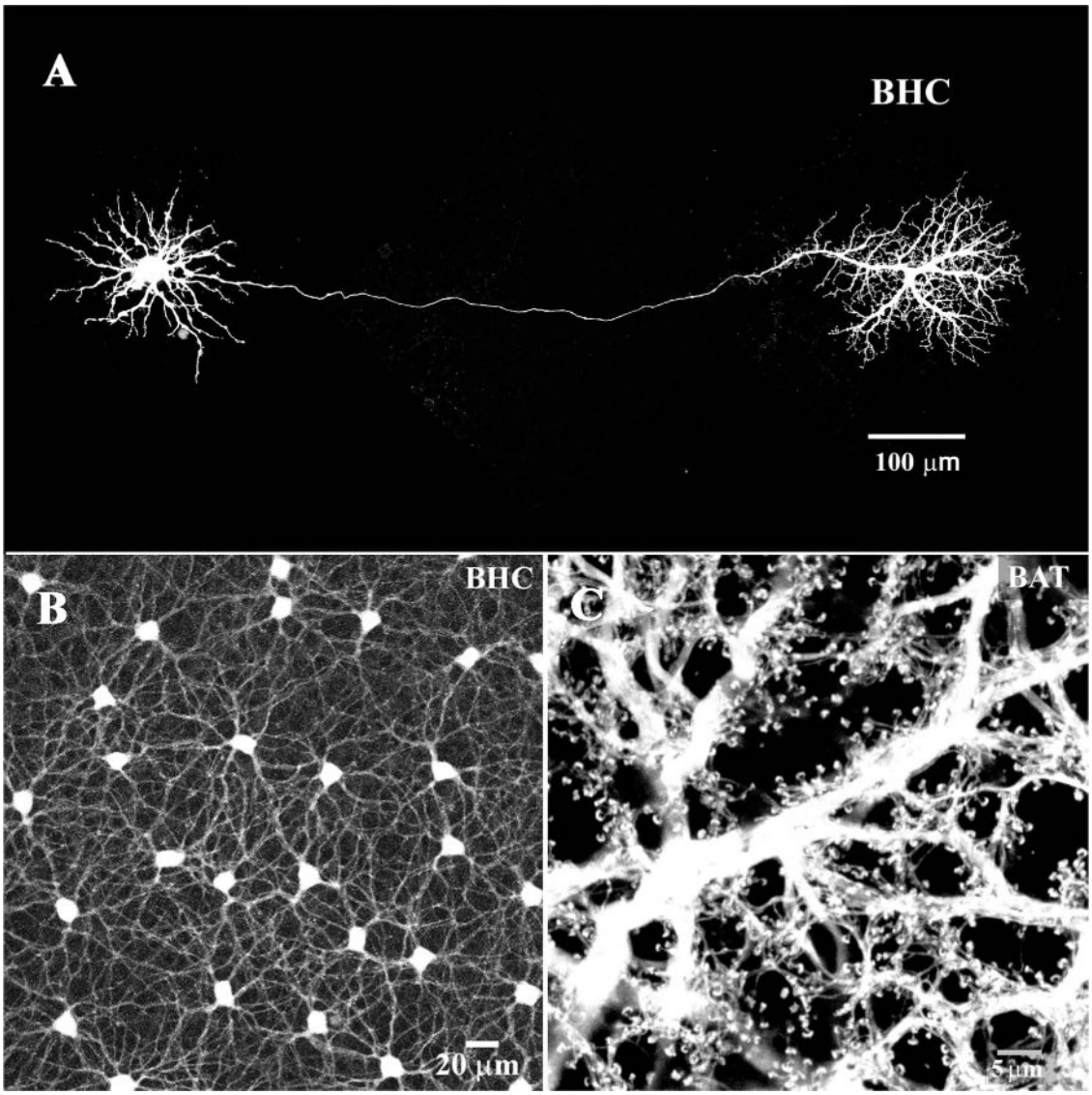

Figure 5.

B-type horizontal cells (HCs). **A**: A single B-type HC was dye injected with Neurobiotin in the presence of meclofenamic acid (MFA, 200 μM), to block gap junctions (Pan and Massey, 2007). Under these conditions, a single axon-bearing HC was obtained. The cell body, with somatic dendrites is on the left, connected by a very fine axon to the axon terminal, on the right. **B**: In the absence of MFA, when a B-type HC was dye injected the mosaic of dye-coupled somas was obtained connected by a plexus of somatic dendrites. **C**: In contrast, when an axon terminal was dye-injected a field of overlapping axon terminals was filled. Note the absence of cell bodies and the characteristic fine endings which contact individual rod spherules.

Author Manuscript Author Manuscript Author Manuscript Author Manuscript

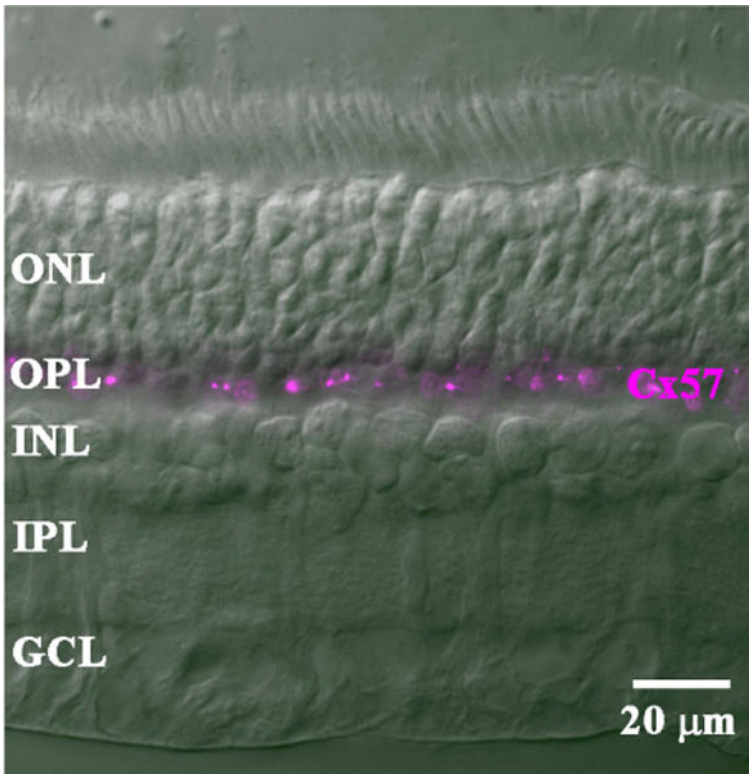

Figure 6.

Cx57 labeling of a cross-section of rabbit retina. In a DIC image, the layers of the rabbit retina were clearly visible. Staining with the mouse Cx57 antibody labeled bright clusters confined to the OPL. The rest of the retina was unlabeled.

Author Manuscript Author Manuscript Author Manuscript Author Manuscript

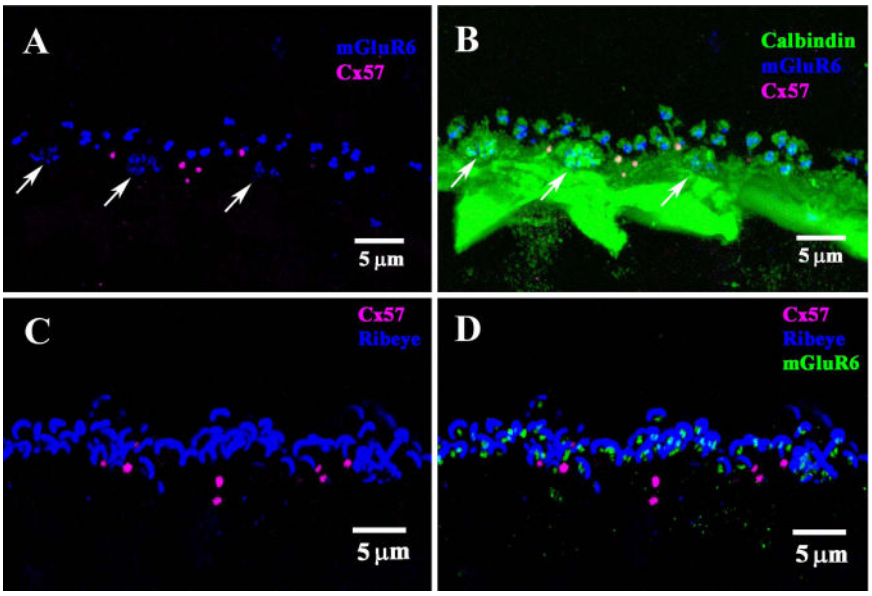

Figure 7.

Comparison of Cx57 labeling with other neuronal markers. **A**: Double label of vertical section of rabbit retina showed punctate labeling of Cx57 (magenta) in the OPL. Staining for mGluR6 (blue) produced clusters of fine ON bipolar terminals (arrows), which indicate the location of cone pedicles, and larger pairs of rod bipolar terminals, which show the location of rod spherules. The Cx57 plaques were below the level of the rod terminals, but occasionally above the level of the cone pedicles, as previously reported by Puller et al. (2009). This suggests an association with the ATs which also run at this level. **B**: Triple label image, with horizontal cells (HCs) stained with an antibody against calbindin (green). A very dense band was stained with a prominent cluster of HC terminals which converge at the site of each cone pedicle (arrows). Very fine HC processes left the plexus to contact each rod spherule, surrounding bright mGluR6 doublets. The Cx57 plaques lie at the top of the HC band mostly below the photoreceptor terminal. There was no apparent relationship between the Cx57 plaques and either cone pedicles or rod spherules. **C**: Double label image showing Cx57 plaques (magenta) and synaptic ribbons in the OPL stained for RIBEYE (blue). Many large curved rod synaptic ribbons were stained. **D**: Triple label image with mGluR6 receptors (green) nestled within each synaptic ribbon. As above, there was no apparent relationship between Cx57 and photoreceptor terminals. The Cx57 plaques were mostly below the level of photoreceptor terminals.

Author Manuscript Author Manuscript Author Manuscript Author Manuscript

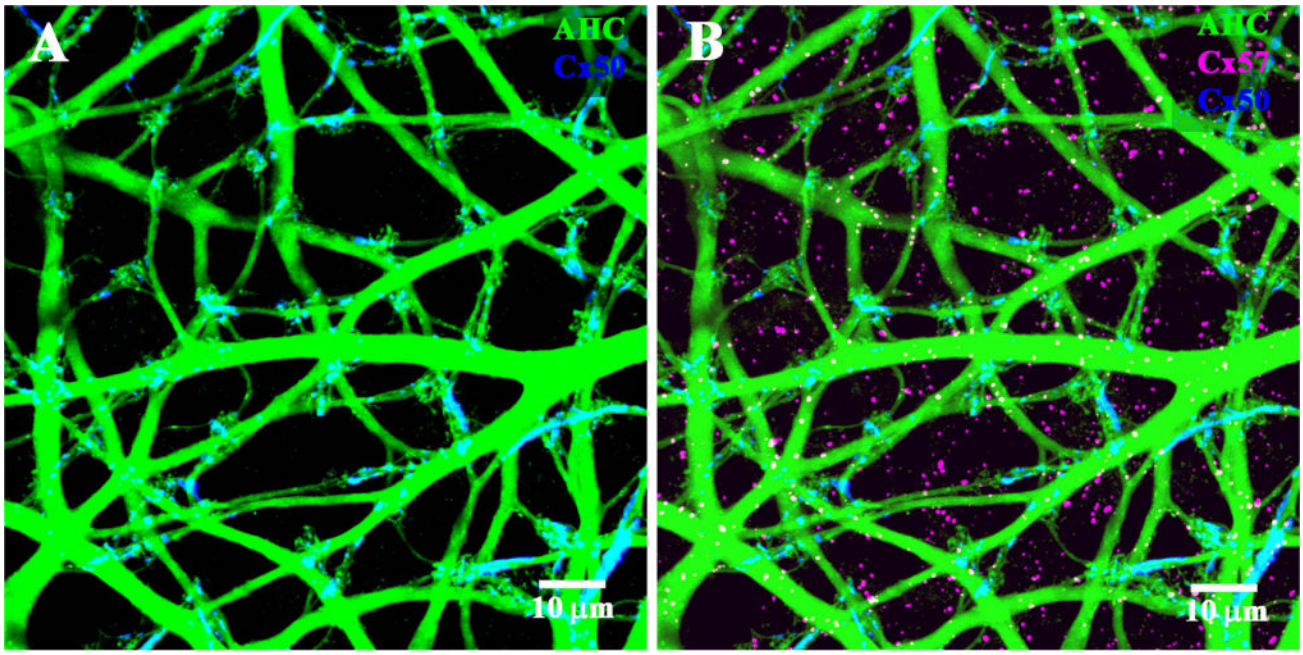

Figure 8.

Connexin labeling of A-type horizontal cells (HCs). **A**: The A-type HC plexus (green) was filled by dye injection with Neurobiotin. Double labeling showed that Cx50 plaques (blue) were colocalized with the A-type HC plexus. **B**: In contrast, Cx57 labeling (magenta) was not associated with A-type HCs or Cx50 plaques.

Author Manuscript Author Manuscript Author Manuscript Author Manuscript

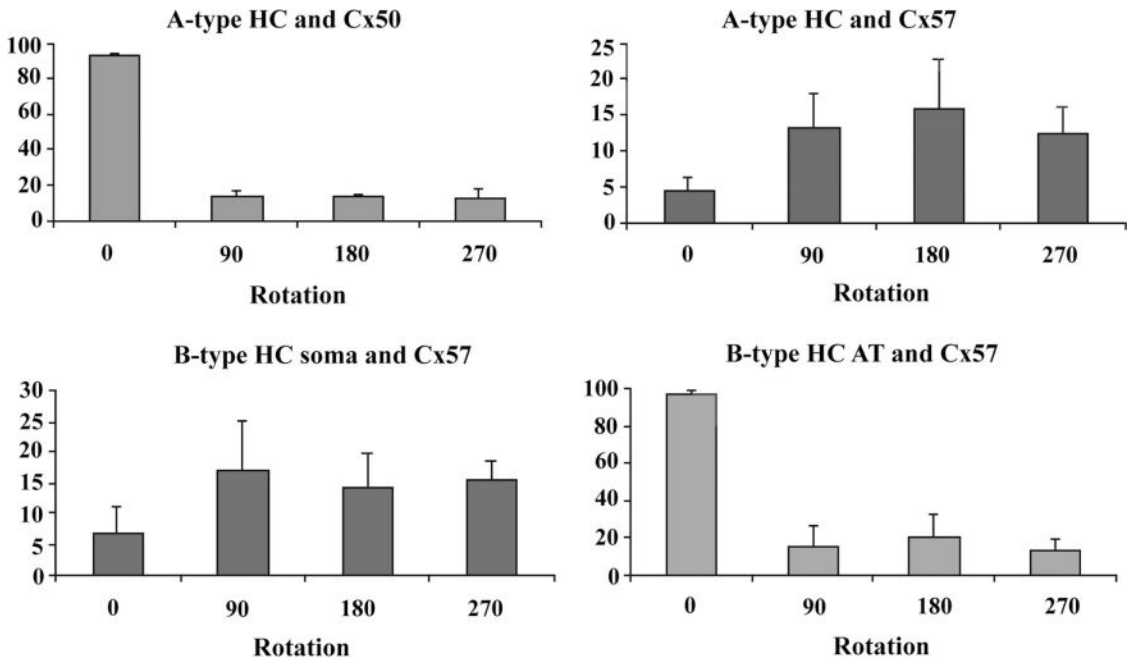

Figure 9.

Rotational analysis from single confocal sections. **A**: A-type HCs and Cx50. In the original orientation ≈92% of Cx50 plaques were associated with A-type HCs. When one channel was rotated through 90, 180, or 270°, the apparent colocalization decreased dramatically to less than 20%. **B**: In contrast, less than 5% of Cx57 plaques were associated with A-type HCs in the control orientation. Upon rotation, the degree of colocalization actually rose to ≈15%, higher than the original orientation. This indicates that Cx57 gap junctions are anticorrelated with A-type HCs. C: B-type HC somatic dendrites and Cx57. Approximately 5% of Cx57 plaques were colocalized with B-type somatic dendrites and rotation substantially increased the apparent colocalization to 15%. This is the same signature as for Cx57 and A-type HCs, indicating anticorrelation between Cx57 and the somatic plexus of B-type HCs. **D**: Cx57 and the B-type AT plexus. Over 90% of Cx57 plaques were colocalized with the AT plexus. Rotation decreased this fraction dramatically. This is the same signature as for Cx50 and A-type HCs, which indicates that Cx57 was truly colocalized with the B-type AT plexus.

Author Manuscript Author Manuscript Author Manuscript Author Manuscript

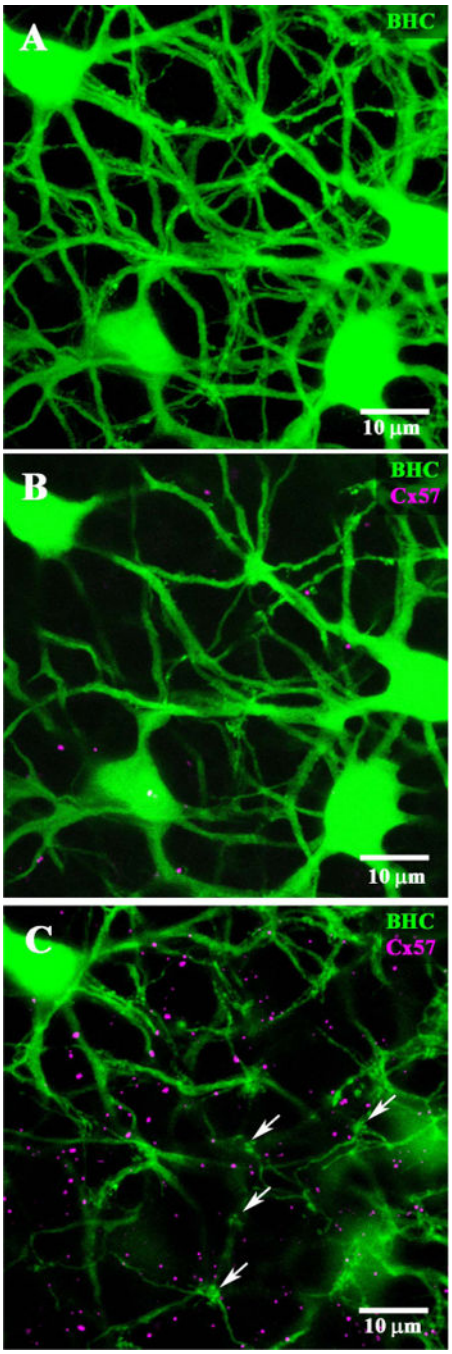

Figure 10.

Cx57 and B-type horizontal cells (HCs). **A**: The cell bodies and somatic dendrites of B-type HCs were filled with Neurobiotin (green). The top panel shows a wholemount confocal stack through the OPL. The cell bodies of several B-type HCs are present and a plexus of somatic dendrites but there are no fine processes characteristic of the axon terminal plexus. **B**: A single confocal section close to the depth of the cell bodies showing the major dendrites. Cx57 plaques (magenta) were not associated with the somatic dendrites of B-type HCs. **C**: Another single confocal section, at a slightly higher plane of focus. Terminal

clusters of somatic dendrites (arrows) show the sites of individual cone pedicles. At this level, high in the OPL, Cx57 plaques are much more numerous but they appear to be independent of the B-type HC somatic dendrites.

Author Manuscript Author Manuscript Author Manuscript Author Manuscript

Author Manuscript Author Manuscript Author Manuscript Author Manuscript

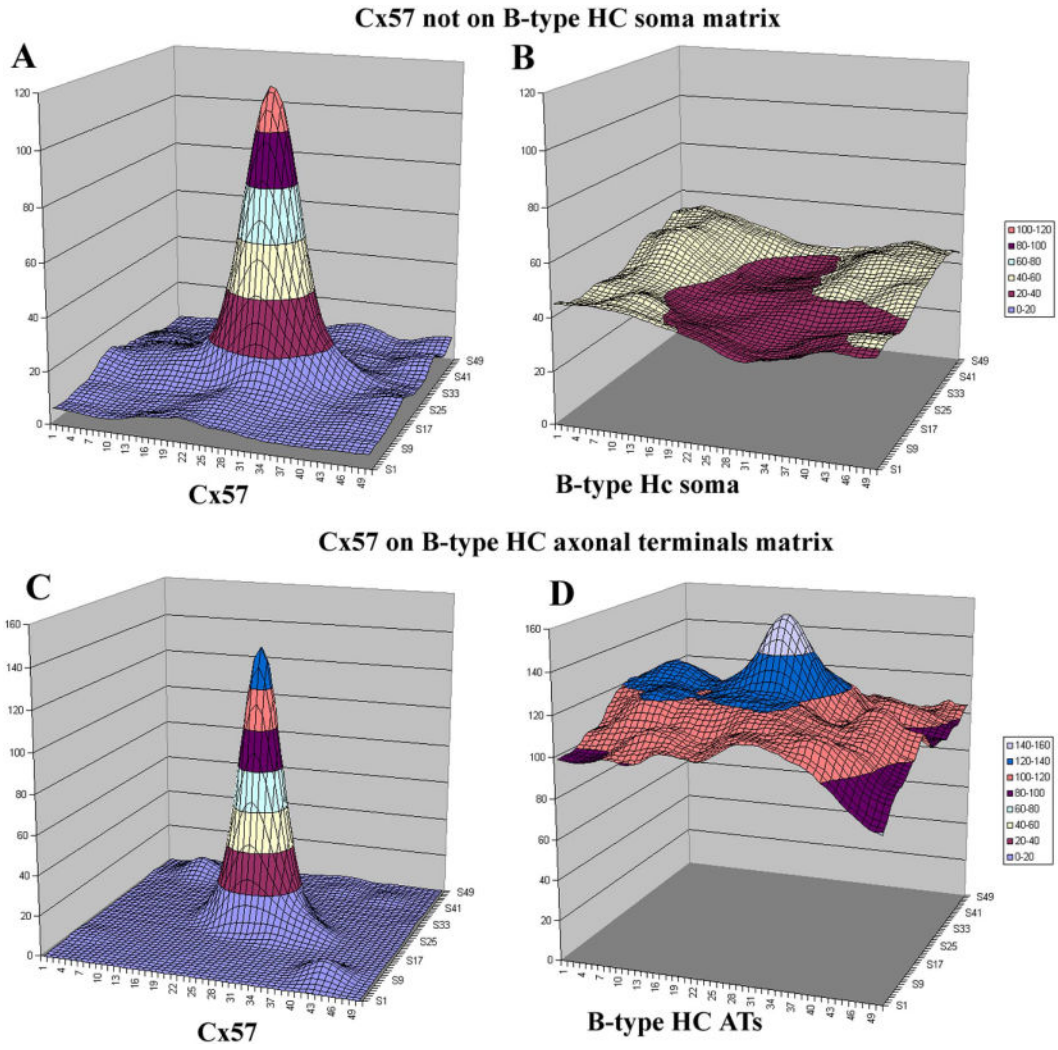

Figure 11.

Image analysis for Cx57. **A**: A 2-μm sampling box was centered over every Cx57 plaque in a single confocal image of the rabbit OPL. Aligning and signal averaging for the Cx57 plaques produced a strong central peak, as expected. **B**: The average distribution of a second channel, labeled for B-type somatic dendrites, around the central Cx57 peak. There was a central depression in the distribution of B-type somatic dendrites indicating anticorrelation with Cx57 gap junctions. **C**: The Cx57 peak obtained after selecting the Cx57 plaques in a single confocal image. **D**: The average distribution of the second cannel, labeled for the axon terminal plexus. There is a prominent peak in the center of the plot. This indicates there is a high probability that an axon terminal process is associated with each Cx57 plaque.

Author Manuscript
Author Manuscript
Author Manuscript
Author Manuscript

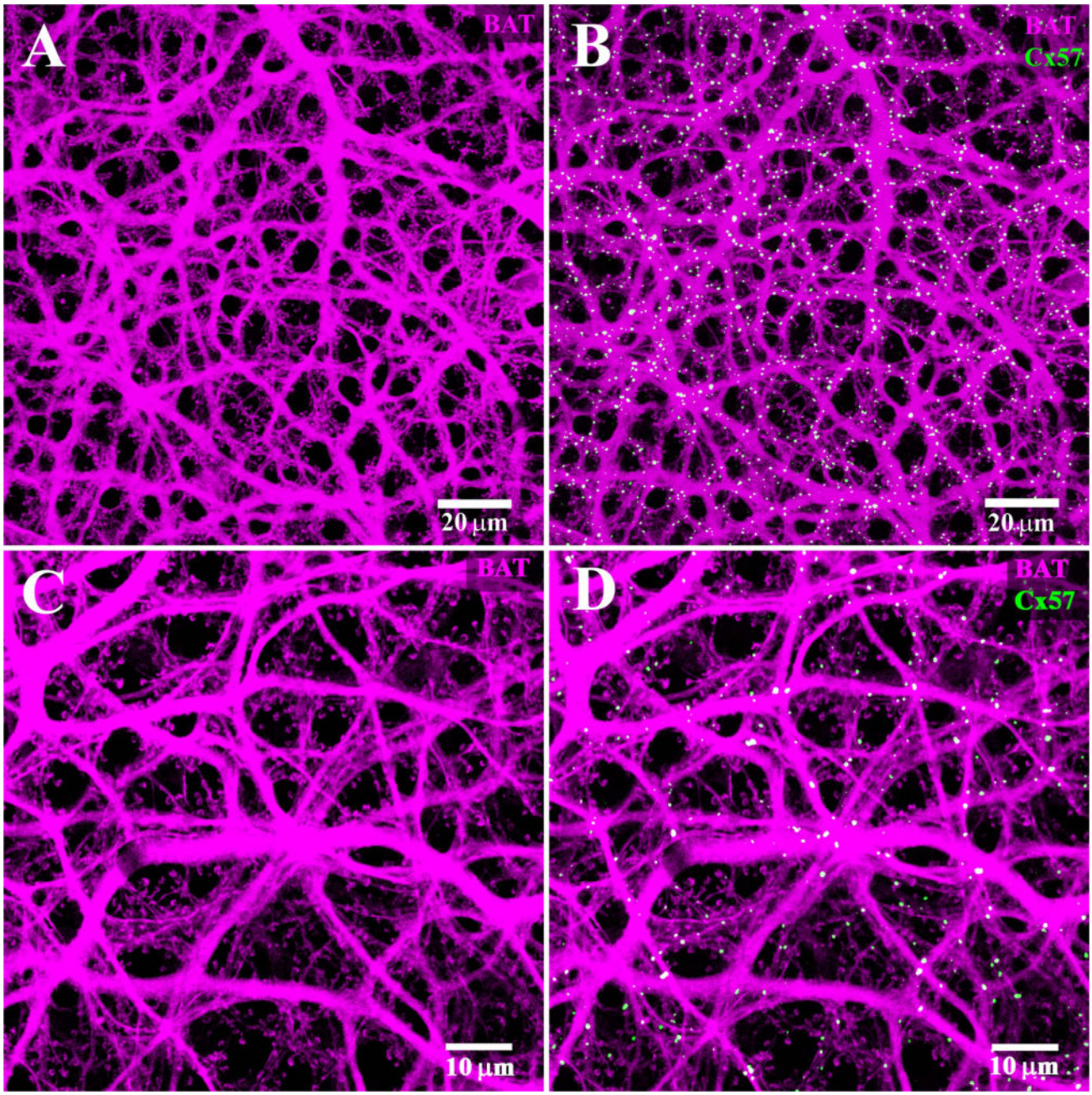

Figure 12.

B-type axon terminal plexus. **A**: The B-type AT plexus was filled with Neurobiotin (magenta). There are numerous fine endings which contact individual rod spherules and a complete absence of cell bodies. This indicates that the B-type AT plexus is labeled exclusively. **B**: The Cx57 plaques (green) are found colocalized with the B-type AT plexus. Note the Cx57 plaques appear almost exclusively white and there are almost no green, single-labeled plaques. **C**: High-magnification view of the AT plexus. The absence of B-type somas and the presence of numerous typical AT endings to match the distribution of

rod spherules indicate that only the AT processes were labeled. **D**: Same frame, nearly all the Cx57 plaques are colocalized with the AT plexus.

Author Manuscript Author Manuscript Author Manuscript Author Manuscript

Author Manuscript Author Manuscript Author Manuscript Author Manuscript

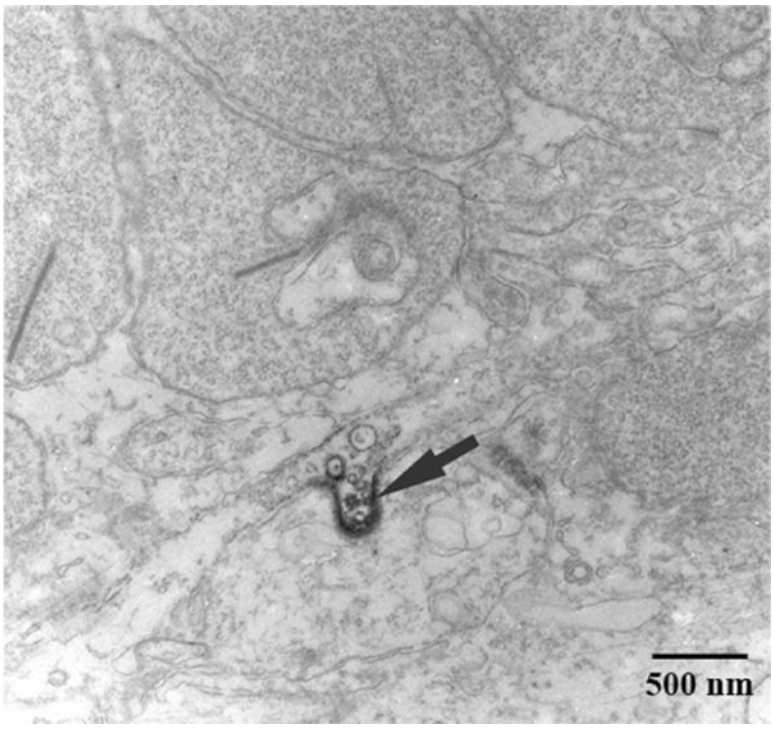

Figure 13.

Electron microscopy for Cx57. The figure shows a region of the outer plexiform layer (OPL). The profiles at the top of the frame are rod spherules, as shown by the prominent synaptic ribbons and numerous synaptic vesicles. Cx57 immunoreactivity was found between two profiles. This putative Cx57 gap junction (arrow) has an invaginating profile. As previously noted for the confocal images, there was no evidence of Cx57 labeling associated with rod spherules.

Author Manuscript

Author Manuscript

Author Manuscript

Author Manuscript

TABLE 1

Antibodies Used and Their Immunogens, Suppliers, and Dilutions

Antigen	Immunogen	Manufacturer, catalog number, species, type	Dilution
Cx57	C-terminal a.a. 414–430 (CRESGGWVDKSRPGSRKA) of rabbit Cx57	Massey lab, rabbit polyclonalMassey lab, mouse monoclonal	1:100 1:100
GFP	Full-length *Aequorea victoria* green fluorescent protein	Clontech (Mountain View, CA) # 632381, mouse monoclonal	1:100
Cx57 mid	Mouse Cx57 a.a. 248–263	Invitrogen (Zymed, Camarillo, CA) #40-5000, rabbit polyclonal	1:100
Cx57 C-terminal	Mouse Cx57 a.a. 434–446	Invitrogen (Zymed, Camarillo, CA), #40-4800, rabbit polyclonal	1:100
mGluR6	Rabbit C-terminus (KTTSTVAAPPKGADTEDPK) Rabbit N-terminus (KLTSSGGQSDEATR)	Massey lab, rabbit polyclonal Massey lab, goat polyclonal	1:1,000
RIBEYE	CtBP2 C-term. a.a. 361-445	BD Biosciences (San Jose, CA) #612044, mouse monoclonal	1:500
Calbindin D-28 (CB) Cx50	Recombinant rat calbindin 19 a.a. C-terminal of mouse Cx40	Swant (Switzerland) #CB38, rabbit polyclonal, Chemicon/Millipore AB1726	1:5,000 1:500